Multiresolution decomposition of quantum field theories using wavelet bases

Tracie Michlin

Department of Applied Mathematics and Computational Science, The University of Iowa, Iowa City, Iowa 52242, USA

W. N. Polyzou

Department of Physics and Astronomy, The University of Iowa, Iowa City, Iowa 52242, USA

Fatih Bulut

Department of Physics, Inönü University, Malatya 44280, Turkey

(Received 1 November 2016; published 1 May 2017)

We investigate both the theoretical and computational aspects of using wavelet bases to perform an exact decomposition of a local field theory by spatial resolution. The decomposition admits natural volume and resolution truncations. We demonstrate that flow equation methods can be used to eliminate short-distance degrees of freedom in truncated theories. The method is tested on a free scalar field in one dimension, where the spatial derivatives couple the degrees of freedom on different scales, although the method is applicable to more complex field theories. The flow equation method is shown to decouple both distance and energy scales in this example. The response to changing the volume and resolution cutoffs and the mass is discussed.

DOI: 10.1103/PhysRevD.95.094501

I. INTRODUCTION

In this paper we investigate the use of wavelet methods [1–20] to decouple degrees of freedom on different distance scales in local quantum field theory. The Daubechies wavelets and scaling functions can be used to construct an orthonormal basis of compactly supported functions [21–35]. The basis includes functions that vanish outside of any arbitrarily small open set. They are generated from a single function using translations and unitary scale transformations. These basis functions decompose the Hilbert space into a direct sum of orthogonal subspaces associated with different resolutions. Expanding local fields in this basis leads to an exact representation of the field as an infinite linear combination of operators with different spatial resolutions. This expansion replaces the operator-valued distributions by infinite linear combinations of basis functions with operator-valued coefficients. The operator-valued coefficients are defined by smearing the local fields with the basis functions. While the full expansion is exact, there are natural volume and resolution truncations that are defined by retaining only terms in the expansion that have support intersecting a given volume and with a specified finest resolution.

We limit our considerations to the use of Hamiltonian methods; however the representations used in this paper could also be employed in any field theory framework to provide natural volume and resolution truncations. They could also be utilized in alternative wavelet approaches [8,10,12,13,16–18]. When the fields are replaced by these expansions in field-theory Hamiltonians, local products of field operators are replaced by infinite linear combinations of products of well-defined operators. The singularities that arise from the local operator products reappear as non-convergence of sums, so the renormalization problem takes on a different form. The theory is naturally regularized by truncating the basis in both resolution and volume.

The problem of constructing a local limit involves first solving the field equations for truncated theories with different volume and resolution cutoffs and adjusting the dimensionless parameters of each truncated field theory to preserve some common observables. Since the truncated theories are systems with a finite number of degrees of freedom, they can in principle be solved, just like lattice truncations. The problem is to identify a sequence of truncated theories and a limiting procedure that results in a well-defined infinite-volume, infinite-resolution limit that satisfies the axioms of a local field theory. The general existence of such a limit is an unsolved problem, and is beyond the scope of this paper.

However, for measurements involving a fixed energy scale and finite volume, the number of relevant degrees of freedom is finite. Under these conditions both the accessible volume and resolution are limited. Truncated field theories that include degrees of freedom associated with this volume and resolution should describe physics on this scale after determining the parameters of the truncated theory by experiment. The predictions at this scale should be improvable as the volume and resolution are increased by finite amounts. This is independent of the existence of an infinite-volume, infinite-resolution limit that describes physical phenomena on all scales.

While it is possible to work at successively finer resolutions, there are reasons to eliminate short-distance degrees of freedom that are much smaller than the scales accessible to a given experiment. This reduces the number of degrees of freedom, where the effects of the eliminated degrees of freedom appear in a more complicated effective Hamiltonian that only involves the physically relevant degrees of freedom. This is similar in spirit to the program initiated by Glöckle and Müller to eliminate explicit pion degrees of freedom in a field theory of interacting pions and nucleons [36] using an "Okobu" transformation [37].

A feature of the wavelet representation is that the commutation relations among the field operators are all discrete, and there are irreducible canonical pairs of operators associated with each resolution and volume. The truncated Hamiltonians with different resolutions have the same form, with coefficients that are rescaled as a function of the resolution. There is a natural transformation that transforms the high-resolution truncated Hamiltonian to the sum of the corresponding low-resolution truncated Hamiltonian and corrections that involve the missing high-resolution degrees of freedom. These corrections include operators that couple the high- and low-resolution degrees of freedom.

Block diagonalizing this Hamiltonian according to resolution gives an effective Hamiltonian entirely in the low-resolution degrees of freedom that includes the physics of the eliminated high-resolution degrees of freedom. This can be compared to the original low-resolution Hamiltonian to see how it must be modified to include the effects of the eliminated degrees of freedom. In this representation explicit high-resolution degrees of freedom are replaced by more complicated effective interactions in the low-resolution degrees of freedom. While this process generates new effective operators, the coefficients of these operators are well-defined functions of the parameters of the original theory, so in a renormalizable theory there is no need to introduce new parameters associated with the new effective operators, although this can always be done to improve convergence.

In this paper we investigate the use of flow equation methods [38–46] to perform the block diagonalization of the high-resolution Hamiltonian. In general the flow equation will generate an infinite collection of complicated effective operators. In order to separate the problem of convergence of the flow equation from an analysis of the scaling properties of the effective interactions, we consider the case of a free field. For free fields the different resolution degrees of freedom are coupled by spatial derivatives, but the structure of the operators generated by the flow equation remain quadratic functions of the fields, which restricts the structure of the operators that are generated by the flow equation to a finite number of classes. Because of this, the flow equation can be solved without addressing the problem of how to manage the generated effective interactions. This provides a first test of the proposed flow equation method to separate scales.

II. BACKGROUND: WAVELET BASIS

In this section the basis of functions that will be used to expand the field operators are defined. The basis functions on the real line are the Daubechies scaling functions [21,22,30,32–34] on a fixed scale and the Daubechies wavelets on all smaller scales.

Our preference for the Daubechies basis is because the basis functions are orthonormal and have compact support. The scale is associated with the size of the support of different basis functions. In higher dimensions the basis functions are products of the one-dimensional basis functions defined in this section. This leads to a representation of the theory in terms of local observables. The structure of the truncated theory is similar to lattice truncations which are also formulated in terms of local degrees of freedom. One advantage of wavelet truncations is that it is possible to include independent degrees on different scales, so large-scale degrees of freedom do not have to be generated by the collective dynamics of many small-scale degrees of freedom.

One useful property of the scaling-wavelet basis is that all of the basis functions can be constructed from a single function, $s(x)$, called the scaling function, by integer translations and dyadic scale transformations. The scaling function, $s(x)$, is the solution of the following linear renormalization group equation:

$$s(x) = \underbrace{S\underbrace{\left(\sum_{l=0}^{2K-1} h_l T^l s(x)\right)}_{\text{block average}}}_{\text{rescale}}. \tag{1}$$

The normalization of the solution of this homogeneous equation is fixed by the condition

$$\int dx s(x) = 1. \tag{2}$$

In Eq. (1) T is a unitary integer translation operator and S is a unitary scale transformation operator that shrinks the support of a function by a factor of 2. These operators are

$$Ts(x) = s(x-1) \qquad Ss(x) = \sqrt{2}s(2x). \tag{3}$$

Equation (1) implies that $s(x)$ is the fixed point of the operation of taking a weighted average of a finite number of translated copies of $s(x)$ scaled to half of the original support. K is a fixed integer that is related to the smoothness of the basis functions. The weights, h_l, are real numbers determined by the three conditions:

(1) Orthonormality of integer translations of $s(x)$:

$$\int s(x)s(x-n)dx = \delta_{n0}. \tag{4}$$

TABLE I. Scaling coefficients for the Daubechies $K=3$ wavelets.

h_0	$(1+\sqrt{10}+\sqrt{5+2\sqrt{10}})/16\sqrt{2}$
h_1	$(5+\sqrt{10}+3\sqrt{5+2\sqrt{10}})/16\sqrt{2}$
h_2	$(10-2\sqrt{10}+2\sqrt{5+2\sqrt{10}})/16\sqrt{2}$
h_3	$(10-2\sqrt{10}-2\sqrt{5+2\sqrt{10}})/16\sqrt{2}$
h_4	$(5+\sqrt{10}-3\sqrt{5+2\sqrt{10}})/16\sqrt{2}$
h_5	$(1+\sqrt{10}-\sqrt{5+2\sqrt{10}})/16\sqrt{2}$

(2) Consistency:

$$\sum_{l=0}^{2K-1} h_l = \sqrt{2}. \quad (5)$$

(3) Ability to locally pointwise represent low-degree polynomials:

$$x^n = \sum_{m=--\infty}^{\infty} c_m s(x-m) \qquad 0 \le n \le K. \quad (6)$$

Although the sum in (6) is infinite, there are no convergence problems because only a finite number of terms in this sum are nonzero at any given point.

There are two solutions of Eqs. (4)–(6) for the h_l. They are related by $h'_l = h_{2K-1-l}$. The corresponding fixed points, $s(x)$, are mirror images of each other. The resulting $s(x)$ has compact support on the finite interval $[0, 2K-1]$. The values for $K=3$, which are used in this work, are given in Table I. These h_l values are simple algebraic numbers.

Scaling functions are defined by translating and rescaling $s(x)$:

$$s_n^k(x) \coloneqq S^k T^n s(x) = 2^{k/2} s(2^k(x - 2^{-k}n)). \quad (7)$$

It follows from (4) and the unitarity of S that the functions $s_n^k(x)$ are orthonormal for each fixed k.

Subspaces $\mathcal{S}_k(\mathbb{R}) \subset L^2(\mathbb{R})$ of resolution $1/2^k$ are defined by

$$\mathcal{S}_k \coloneqq \{f(x) | f(x) = \sum_{n=-\infty}^{\infty} c_n s_n^k(x), \qquad \sum_{n=-\infty}^{\infty} |c_n|^2 < \infty\}.$$

It follows from (1) that these subspaces are related by

$$\mathcal{S}_k \coloneqq S^k \mathcal{S}_0 \qquad \mathcal{S}_k \subset \mathcal{S}_{k+n} \qquad n \ge 0$$

or more generally they are nested:

$$\cdots \mathcal{S}_{k-1} \subset \mathcal{S}_k \subset \mathcal{S}_{k+1} \subset \cdots. \quad (8)$$

The inclusions in (8) are proper in the sense that they have nonempty orthogonal complements:

$$\mathcal{S}_{k+1} = \mathcal{S}_k \oplus \mathcal{W}_k \qquad \mathcal{W}_k \neq \{\emptyset\}.$$

The space $\mathcal{W}_k$ is the orthogonal complement of $\mathcal{S}_k$ in $\mathcal{S}_{k+1}$. From a physical point of view $\mathcal{S}_{k+1}$ is a finer-resolution subspace than $\mathcal{S}_k$, and $\mathcal{W}_k$ fills in the missing degrees of freedom that are in $\mathcal{S}_{k+1}$ but not in $\mathcal{S}_k$. Combining these decompositions we have the following relation between the subspaces $\mathcal{S}_{k+n}$ and $\mathcal{S}_k$ of different resolutions:

$$\mathcal{S}_{k+n} = \mathcal{S}_k \oplus \mathcal{W}_k \oplus \mathcal{W}_{k+1} \oplus \cdots \oplus \mathcal{W}_{k+n-1}. \quad (9)$$

The limit of this chain as $n \to \infty$ leads to an exact decomposition of $L^2(\mathbb{R})$ by resolution:

$$L^2(\mathbb{R}) = \mathcal{S}_k \oplus \mathcal{W}_k \oplus \mathcal{W}_{k+1} \oplus \mathcal{W}_{k+2} \oplus \mathcal{W}_{k+3} \oplus \cdots. \quad (10)$$

The subspaces $\mathcal{W}_k$ are called wavelet spaces. Orthonormal bases for the subspaces $\mathcal{W}_k$ are constructed from the mother wavelet, $w(x)$, which is defined by taking a different weighted average of translations of the scaling function $s(x)$ scaled to half of the support of $s(x)$:

$$w(x) \coloneqq \sum_{l=0}^{2K-1} g_l S T^l s(x) \qquad g_l = (-)^l h_{2K-1-l}. \quad (11)$$

The weights g_l in Eq. (11) are related to the weights h_l used in (1) except the signs alternate and the order of the indices is reversed.

Applying powers of the dyadic scale transformation operator, S, and integer translation operator, T, to $w(x)$ gives the following basis functions for $\mathcal{W}_k$:

$$w_m^k(x) \coloneqq S^k T^m w(x) = 2^{k/2} w(2^k(x - 2^{-k}m)). \quad (12)$$

The functions $w_m^k(x)$ are called wavelets. It can be shown that for each fixed k, $\{w_m^k(x)\}_{m=-\infty}^{\infty}$ is an orthonormal basis for the subspace $\mathcal{W}_k$. Because of (9) the $w_n^k(x)$ for different values of k are also orthogonal.

From (7), (11), and (12) it follows that both $s_m^k(x)$ and $w_m^k(x)$ can be constructed from the fixed point, $s(x)$, of the renormalization group equation (1), using elementary transformations.

The decomposition (10) implies that for any fixed starting scale 2^{-k},

$$\{s_n^k(x)\}_{n=-\infty}^{\infty} \cup \{w_n^l(x)\}_{n=-\infty, l=k}^{\infty,\infty}$$

is an orthonormal basis for $L^2(\mathbb{R})$ consisting of compactly supported functions. The support of both $s_m^k(x)$ and $w_m^k(x)$ is $[2^{-k}m, 2^{-k}(m+2K-1)]$. For any point on the real line there are basis functions of arbitrarily small support that include that point.

The basis functions $s_n^k(x)$ are associated with degrees of freedom of scale 2^{-k} and the $w_n^l(x)$ are associated with degrees of freedom of scale $2^{-(l+1)}$ that are not of scale 2^{-l}. Thus they are identified with localized degrees of freedom with distance scales 2^{-k-l} for all integers, $l \geq 0$.

Equation (9) implies that the functions

$$\{s_n^{k+m}(x)\}_{n=-\infty}^{\infty} \quad \text{and} \quad \{s_n^k(x)\}_{n=-\infty}^{\infty} \cup \{w_n^l(x)\}_{n=-\infty,l=k}^{\infty,k+m-1}$$

are related by an orthogonal transformation. This transformation is called the wavelet transform. It can be computed more efficiently than a fast Fourier transform, using the h_l and g_l as weights that define "low-pass" and "high-pass" filters:

$$s_n^{k-1}(x) = \sum h_l s_{2n+l}^k(x) \qquad w_n^{k-1}(x) = \sum g_l s_{2n+l}^k(x).$$

The inverse of this orthogonal transformation is

$$s_n^k(x) = \sum_m h_{m-2n} s_m^{k-1}(x) + \sum_m g_{m-2n} w_m^{k-1}(x).$$

It is precisely these transformations (or their three-dimensional generalization) that relate a fine-resolution Hamiltonian to the sum of a coarse-resolution Hamiltonian plus fine scale corrections.

The Daubechies wavelets and scaling functions are fractal functions. This is because $s(x)$ is the solution of a renormalization group equation, and all of the basis functions are obtained by applying a finite number of scale transformations, translations, and sums to $s(x)$. In spite of their fractal nature, these basis functions have a finite number of derivatives that increase with increasing K. This paper uses the $K = 3$ basis. These basis functions have one continuous derivative. This allows for an exact representation of Hamiltonians that have fields with at most one derivative. It explicitly avoids the need for finite difference approximations to derivatives. Increasing K leads to smoother basis functions at the expense of larger support and increasing overlap with basis functions on the same scale.

Quantum fields are generally assumed to be operator-valued tempered distributions. This suggests that field operators smeared with test functions that only have a finite number of derivatives might not be well-defined operators; however free-field Wightman functions smeared with Daubechies $K \geq 3$ wavelets or scaling functions are well defined. This follows from the analytic expressions for the free-field Wightman functions [47] and the fact that the basis functions have compact support and a continuous derivative. This is analogous to the observation that a delta function, which is a distribution, is also a well-defined linear functional on the space of continuous functions. Equation (6) shows that certain linear combinations of these functions can be much smoother. In Ref. [20] it is shown specifically that vacuum expectation values of the Daubechies-wavelet-smeared free fields converge to the exact free-field Wightman functions in the limit of infinite resolution. For theories truncated to a finite number of degrees of freedom, the Stone–von Neumann theorem [48,49], which establishes the unitary equivalence of all representations of the canonical commutation relations, makes it possible to formulate the dynamics of the truncated theory in terms of the well-defined algebra of wavelet-smeared free fields on the free-field Fock space. This ensures that the fractal nature of the basis does not cause any problems in the treatment of the truncated theory. If there are any issues with the fractal nature of the wavelet basis functions, they must arise when one tries to establish the existence of a local limit.

Since the Daubechies basis functions have compact support, their Fourier transforms are analytic. Thus, expanding the field in a coordinate-space wavelet basis is equivalent to expanding the Fourier transform of the field in an analytic basis. The Fourier transformed basis functions are infinitely differentiable. They fall off like inverse powers of the momentum, similar to Feynman diagrams. None of them have compact support.

Another potential issue with fractal basis functions involves their computation. This turns out to be a nonissue because they have compact support and integrals of products of these functions with polynomials of arbitrarily high degree can be computed exactly (reduced to finite linear algebra) using the renormalization group equation (1). Since any continuous function on a compact interval can be approximated by a polynomial, it is possible to accurately compute integrals of products of these basis functions with any continuous function. The renormalization group equation can also be used to reduce the computation of arbitrary products of these basis functions and their derivatives to finite linear algebra. It is even possible to use these methods to evaluate integrals of products of these basis functions with functions having logarithmic or principal-value singularities [32–35]. The computational methods relevant to this work are discussed in the Appendix.

III. WAVELET DISCRETIZED FIELDS

Given a pair of scalar fields $\Phi(x)$ and $\Pi(x)$ satisfying canonical equal-time commutation relations

$$[\Pi(\mathbf{x},t),\Phi(\mathbf{y},t)] = -i\delta(\mathbf{x}-\mathbf{y})$$
$$[\Phi(\mathbf{x},t),\Phi(\mathbf{y},t)] = [\Pi(\mathbf{x},t),\Pi(\mathbf{y},t)] = 0,$$

discrete fields satisfying the discrete form of these commutation relations can be constructed by smearing the spatial coordinates of the fields with an orthonormal set of basis functions.

For the scaling-wavelet basis [we consider the $(1+1)$-dimensional case for notational simplicity] the discrete fields are defined by

$$\Phi^k(s,n,t) \coloneqq \int dx \Phi(x,t) s_n^k(x)$$

$$\Phi^l(w,n,t) \coloneqq \int dx \Phi(x,t) w_n^l(x) \qquad (l \geq k)$$

$$\Pi^k(s,n,t) \coloneqq \int dx \Pi(x,t) s_n^k(x)$$

$$\Pi^l(w,n,t) \coloneqq \int dx \Pi(x,t) w_n^l(x) \qquad (l \geq k).$$

These fields represent degrees of freedom localized on the support of the associated basis function.

As a result of the orthonormality of the basis functions the discrete equal-time commutators are

$$[\Phi^k(s,n,t), \Phi^k(s,m,t)] = 0$$
$$[\Pi^k(s,n,t), \Pi^k(s,m,t)] = 0 \tag{13}$$

$$[\Phi^k(s,n,t), \Pi^k(s,m,t)] = i\delta_{nm} \tag{14}$$

$$[\Phi^r(w,n,t), \Phi^s(w,m,t)] = 0$$
$$[\Pi^r(w,n,t), \Pi^s(w,m,t)] = 0 \tag{15}$$

$$[\Phi^r(w,n,t), \Pi^s(w,m,t)] = i\delta_{rs}\delta_{nm} \tag{16}$$

$$[\Phi^r(w,n,t), \Phi^k(s,m,t)] = 0$$
$$[\Pi^r(w,n,t), \Pi^k(s,m,t)] = 0 \tag{17}$$

$$[\Phi^r(w,n,t), \Pi^k(s,m,t)] = 0$$
$$[\Pi^r(w,n,t), \Phi^k(s,m,t)] = 0. \tag{18}$$

The field operators have the *exact* representation in terms of these discrete operators

$$\Phi(x,t) = \sum_n \Phi^k(s,n,t) s_n^k(x) + \sum_{l\geq k;n} \Phi^l(w,n,t) w_n^l(x) \tag{19}$$

$$\Pi(x,t) = \sum_n \Pi^k(s,n,t) s_n^k(x) + \sum_{l\geq k;n} \Pi^l(w,n,t) w_n^l(x). \tag{20}$$

These expansions can be inserted in the free-field Hamiltonian,

$$H = \frac{1}{2}\int (\Pi(x,0)\Pi(x,0) + \nabla\Phi(x,0)\cdot\nabla\Phi(x,0) + \mu^2\Phi(x,0)\Phi(x,0))dx, \tag{21}$$

which can be expressed exactly in terms of the $t=0$ discrete fields. The discrete form of the exact Hamiltonian is the sum of an operator with only scaling-function fields, H_s; one with only wavelet fields, H_w; and one that has products of both types of fields, H_{sw}:

$$H = H_s + H_w + H_{sw} \tag{22}$$

where

$$H_s \coloneqq \frac{1}{2}\Big(\sum_n \Pi^k(s,n,0)\Pi^k(s,n,0) + \sum_{mn} \Phi^k(s,m,0) D^k_{s;mn} \Phi^k(s,n,0) + \mu^2 \sum_n \Phi^k(s,n,0)\Phi^k(s,n,0)\Big), \tag{23}$$

$$H_w \coloneqq \frac{1}{2}\Big(\sum_{n,l} \Pi^l(w,n,0)\Pi^l(w,n,0) + \sum_{m,l,n,j} \Phi^l(w,m,0) D^{lj}_{w;mn} \Phi^j(w,n,0) + \mu^2 \sum_{l,n} \Phi^l(w,n,0)\Phi^l(w,n,0)\Big),$$

$$H_{sw} \coloneqq \frac{1}{2}\sum_{m,l,n} \Phi^l(w,m,0) D^{lk}_{sw;mn} \Phi^k(s,n,0).$$

The coefficients D^k_{smn}, $D^{lj}_{w,m,n}$ and $D^{lk}_{sw;m,n}$ that couple near neighbor fields and fields with different scales are the constant matrices given by

$$D^k_{s;mn} = \int dx \frac{d}{dx} s_m^k(x) \frac{d}{dx} s_n^k(x) \tag{24}$$

$$D^{lj}_{w;mn} = \int dx \frac{d}{dx} w_m^l(x) \frac{d}{dx} w_n^j(x) \tag{25}$$

$$D^{lk}_{ws;mn} = 2\int dx \frac{d}{dx} w_m^l(x) \frac{d}{dx} s_n^k(x). \tag{26}$$

The support properties of the basis functions imply that the matrices $D^x_{y;mn}$ vanish if the support of the functions in the integrand have empty intersection, so they have a structure similar to a finite difference approximation. For a free field the matrices $D^{lk}_{ws;mn}$ and $D^{lj}_{w,m,n}$ for $l \neq j$ are responsible for the coupling of physical degrees of freedom on different resolution scales. In interacting theories there are additional couplings that come from local products of more than two fields. For example

$$\int \phi^4(x,t)dx = \sum_{n_1n_2n_3n_4} \Gamma^k_{s;n_1\cdots n_4} \Phi^k(s,n_1,t)\Phi^k(s,n_2,t)\Phi^k \times (s,n_3,t)\Phi^k(s,n_4,t) + \cdots$$

where

$$\Gamma^k_{s;n_1\cdots n_4} := \int s^k_{n_1}(x)s^k_{n_2}(x)s^k_{n_3}(x)s^k_{n_4}(x)dx \qquad (27)$$

and the $\cdots$ represent additional terms in the sum that also involve the wavelet basis functions and fields. Like the $D^k_{s;mn}$, the coefficients $\Gamma^k_{s,n_1\cdots n_4}$ are almost local in the sense that they vanish unless all of the functions in the integral (27) have overlapping support. They also include operators that couple degrees of freedom on different scales.

The other important feature of the fractal nature of the scaling-wavelet basis is that these constant coefficients have simple scaling properties. For example

$$D^k_{s;mn} = 2^{2k}D^0_{s;mn} = 2^{2k}D^0_{s;0,n-m} \qquad (28)$$

$$\Gamma^k_{s;n_1\cdots n_4} = 2^k\Gamma^0_{s;n_1\cdots n_4} = 2^k\Gamma^0_{s;0,n_2-n_1,n_3-n_1,n_4-n_1}, \qquad (29)$$

where we have used translational invariance to express these coefficients in terms of $D^0_{s;0,n-m}$ and $\Gamma^0_{s;0,n_2-n_1,n_3-n_1,n_4-n_1}$. In addition, these constant coefficients can all be computed exactly (i.e. reduced to finite linear algebra) using (2)–(3) and the scaling equation (1). This is discussed in detail in [11] and the Appendix. See also [23,24,27,28] for general methods to compute integrals involving wavelets and scaling functions. The result is that for a free field all of the coupling coefficients can be expressed in terms of the nine nonzero coefficients $D^0_{s;0m}$ with $-4 \leq m \leq 4$. These can be computed exactly [11,27]. The results are rational numbers. Their computation is discussed in the Appendix.

IV. FLOW EQUATION

The wavelet basis decomposes the field into a sum of operators that are localized in different finite volumes. Each of these operators are also associated with different resolutions. For free fields the coefficients $D^{kl}_{sw;mn}$, $D^{kl}_{ws;mn}$, and $D^{rs}_{ww;mn}$ in the Hamiltonian couple degrees of freedom with different resolutions.

One can think of $1/2^k$ as the physically relevant resolution scale. The canonical scaling-function fields $\Phi^k(s,n,t)$ and $\Pi^k(s,n,t)$ are an irreducible set of operators for degrees of freedom on this scale. The wavelet fields also appear in the Hamiltonian; they are associated with finer-scale degrees of freedom. Finally products of wavelet and scaling-function fields represent terms that couple degrees of freedom on the physical scale to those on smaller scales.

From a physics point of view, while the smaller scales may not be experimentally relevant, they may represent important contributions to the dynamics. One can imagine integrating them out in a functional integral representation to get an effective theory involving only the experimentally relevant degrees of freedom. This is a difficult calculation in the wavelet representation.

A more direct approach would be to decouple the scaling-function part of the Hamiltonian from the wavelet part. This would also lead to an effective Hamiltonian involving only the physically relevant degrees of freedom $\Phi^k(s,n,t)$ and $\Pi^k(s,n,t)$ and a complementary Hamiltonian that acts only on the remaining degrees of freedom. The decoupling will necessarily generate more complicated effective interactions among the physically relevant degrees of freedom.

We also remark that the free-field Hamiltonian (21) is still a many-body Hamiltonian. Decoupling at the operator level is a stronger condition than decoupling on a finite number of particle subspace.

Flow equations were introduced by Wegner [38] as a method to continuously evolve a Hamiltonian to a unitarily equivalent simpler form. Flow equation methods [39–46] are an alternative to direct diagonalization or block diagonalization methods [37]. They have been applied to problems in quantum field theory and quantum mechanics. They have the advantage that they are simpler to implement than integrating out short-distance degrees of freedom in a functional integral. Flow equations are designed to perform this diagonalization using a continuously parametrized unitary transformation, $U(\lambda)$. The transformed Hamiltonian has the form

$$H(\lambda) = U(\lambda)HU^\dagger(\lambda).$$

Here $H(0) = H$ is the original Hamiltonian; the generator of the flow equation is chosen to continuously evolve the initial Hamiltonian into the desired form as λ increases. Here λ is called the flow parameter. As λ increases from 0 the Hamiltonian evolves towards the desired form. The evolution is constructed to exponentially approach the desired form, but it is possible for the exponent to become small. Nevertheless, evaluating $H(\lambda)$ at any value of λ still yields a Hamiltonian that is unitarily equivalent to the original Hamiltonian with weaker scale-coupling terms.

The preference for flow equation methods in the wavelet representation is that the simple form of the commutators of the discrete canonical fields, (13)–(18), reduces the integration of the flow equation to simple algebra. The problem is to find a generator of the flow that leads to the desired outcome.

In general the unitarity of $U(\lambda)$ implies that it satisfies the differential equation

$$\frac{dU(\lambda)}{d\lambda} = \frac{dU(\lambda)}{d\lambda}U^\dagger(\lambda)U(\lambda) = K(\lambda)U(\lambda)$$

where

$$K(\lambda) = \frac{dU(\lambda)}{d\lambda}U^\dagger(\lambda) = -K^\dagger(\lambda) \qquad (30)$$

is the anti-Hermitian generator of this unitary transformation. We are free to choose a generator that leads to the desired outcome. It follows that $H(\lambda)$ satisfies the differential equation

$$\frac{dH(\lambda)}{d\lambda} = [K(\lambda), H(\lambda)].$$

For this application it is useful to choose a generator, $K(\lambda)$, that is a function of the evolved Hamiltonian:

$$K(\lambda) = [G(\lambda), H(\lambda)] \tag{31}$$

where $G(\lambda)$ is the part of $H(\lambda)$ with the operators that couple different scales turned off. With this choice $G(\lambda) = G^{\dagger}(\lambda)$ so $K(\lambda)$ is anti-Hermitian.

It follows that

$$\begin{aligned}\frac{dH(\lambda)}{d\lambda} &= [K(\lambda), H(\lambda)] = [[G(\lambda), H(\lambda)], H(\lambda)] \\ &= [H(\lambda), [H(\lambda), G(\lambda)]].\end{aligned} \tag{32}$$

Equation (32) is the desired flow equation for our free-field Hamiltonian. A fixed point, λ^*, of this equation occurs when

$$[H(\lambda^*), [H(\lambda^*), G(\lambda^*)]] = 0.$$

It follows from the structure of the equation that the generator $K(\lambda)$ only contains operators that couple the wavelet and scaling-function degrees of freedom. Below we discuss the argument that this nonlinear equation drives this commutator to zero for the case of a free-field Hamiltonian.

The following considerations are limited to the case of a free field. This is because for interacting fields integrating the flow equation generates an infinite number of new operators. The nonzero commutators of polynomials of field operators of degree n and m are polynomials of degree $n + m - 2$. Each iteration of the flow equation increases the degree of the polynomials. The new operators represent many-body interactions in the transformed Hamiltonian. A separate analysis of the scaling properties of these many-body polynomial operators is needed to determine the relative strength of these operators, and which, if any, operators can be safely discarded. This analysis is separate from considerations about the flow equation and needs to be developed in applications to realistic systems.

To understand what happens in the case of the free-field Hamiltonian (21) first note that for the starting Hamiltonian all of the operators are quadratic in the $\Phi^k(s/w, n, t)$ and $\Pi^k(s/w, n, t)$ operators, and commutators of these quadratic polynomials remain quadratic polynomials. The decomposition $H(\lambda) = G(\lambda) + H_{sw}(\lambda)$ implies that the right hand side of equation (32) can be expressed as a sum of two terms, $[G(\lambda), [H_{sw}(\lambda), G(\lambda)]]$ and $[H_{sw}(\lambda), [H_{sw}(\lambda), G(\lambda)]]$. An examination of the operator structure of each of these terms indicates that the first term only contains operators the couple the two scales while the second term only contains operators that preserve scales. Likewise the commutator of different scale-coupling operator parts gives zero or a product of two scaling or two wavelet function operators. This allows us to separate the flow equation into separate equations for the scale-coupling term $H_{sw}(\lambda)$ and uncoupled terms $G(\lambda) = H_s(\lambda) + H_w(\lambda)$. Defining

$$H_A(\lambda) = G(\lambda) \qquad H_B(\lambda) = H_{sw}(\lambda),$$

the flow equations can now be separated into coupled equations for the mixed (B) and nonmixed (A) parts of the Hamiltonian:

$$\begin{aligned}\frac{dH_A(\lambda)}{d\lambda} &= [H_B(\lambda), [H_B(\lambda), H_A(\lambda)]], \\ \frac{dH_B(\lambda)}{d\lambda} &= [H_A(\lambda), [H_B(\lambda), H_A(\lambda)]] \\ &= -[H_A(\lambda), [H_A(\lambda), H_B(\lambda)]].\end{aligned}$$

These equations have a symmetric form under $H_A(\lambda) \leftrightarrow H_B(\lambda)$ except for a sign, which can be seen by changing the order in the commutator in the second equation.

To understand how these equations evolve the Hamiltonian to the desired form, we express the first equation in a basis of eigenstates of $H_B(\lambda)$ with eigenvalues $e_{bn}(\lambda)$ and the second in a basis of eigenstates of $H_A(\lambda)$ with eigenvalues $e_{an}(\lambda)$. The equations for the matrix elements in each of these bases have the form

$$\frac{dH_{Amn}(\lambda)}{d\lambda} = (e_{bm}(\lambda) - e_{bn}(\lambda))^2 H_{Amn}(\lambda) \tag{33}$$

and

$$\frac{dH_{Bmn}(\lambda)}{d\lambda} = -(e_{am}(\lambda) - e_{an}(\lambda))^2 H_{Bmn}(\lambda). \tag{34}$$

These equations can be integrated exactly:

$$H_{Amn}(\lambda) = e^{\int_0^{\lambda}(e_{bm}(\lambda') - e_{bn}(\lambda'))^2 d\lambda'} H_{Amn}(0) \tag{35}$$

$$H_{Bmn}(\lambda) = e^{-\int_0^{\lambda}(e_{am}(\lambda') - e_{an}(\lambda'))^2 d\lambda'} H_{Bmn}(0). \tag{36}$$

These solutions show that matrix elements of H_A increase exponentially while matrix elements of H_B decrease exponentially as the flow parameter λ is increased. This evolution can stall if there are degeneracies in the eigenvalues, if there are approximate degeneracies, or if the eigenvalues cross for some value of λ.

It is also apparent from these equations that in the high-resolution, large-volume limit, where the spectrum of the block diagonal operators approaches a continuous spectrum, there will be closely spaced eigenvalues, which will lead to slow convergence of some parts of the scale-coupling operator.

To solve these equations numerically the Hamiltonian needs to be truncated to a finite number of degrees of freedom. This means that it is necessary to truncate both the volume and resolution. Any system with a finite energy in a finite volume is expected to be dominated by a finite number of degrees of freedom [50]. These can be separated into degrees of freedom associated with an experimental scale and additional relevant degrees of freedom at smaller scales. We can use scaling-function fields as the degrees of freedom on the experimental scale and wavelet degrees of freedom on the smaller scales that are still relevant to the given volume and energy scale.

While similar remarks apply to Hamiltonians with interactions, in general a different flow generator may be needed to separate the different-scale degrees of freedom. It may also be necessary to first project the truncated Hamiltonian on a subspace before solving the flow equation.

V. TEST

To determine if solving the flow equation eliminates the coupling terms, we consider a truncation of the free-field Hamiltonian (21) to a finite volume with two resolutions, using 32 basis functions: 16 scaling functions and 16 wavelets to expand the fields. For simplicity, we only keep wavelets on one scale. The coefficients $D^{k}_{s;mn}$, $D^{lj}_{w;mn}$, and $D^{lk}_{sw;mn}$, in (24), (25), and (26) are given in [11] and computed in the Appendix. The truncated fields are defined by an expansion in a finite number of basis functions of two resolutions:

$$\Phi(x) = \sum_{n=0}^{15} s_n(x)\Phi(s,n,t) + \sum_{n=0}^{15} w_n(x)\Phi(w,n,t) \tag{37}$$

$$\Pi(x) = \sum_{n=0}^{15} s_n(x)\Pi(s,n,t) + \sum_{n=0}^{15} w_n(x)\Pi(w,n,t). \tag{38}$$

The truncated fields in (37) and (38) vanish smoothly at $x = 0$ and $x = 20$, corresponding to the edge of the support of the leftmost and rightmost basis functions. While a more complicated boundary condition could be used, this choice is the most straightforward to implement, and corresponds to the projection of the wavelet basis on a finite-dimensional subspace.

The truncated Hamiltonian is constructed by inserting these truncated fields in the free-field Hamiltonian. The resulting Hamiltonian is quadratic in these fields, and has the form

$$\begin{aligned} H = {}& \sum_{mn} a_{ssmn}(\lambda)\Phi(s,m,0)\Phi(s,n,0) + \sum_{mn} b_{ssmn}(\lambda)\Pi(s,m,0)\Pi(s,n,0) \\ &+ \sum_{mn} c_{ssmn}(\lambda)\Phi(s,m,0)\Pi(s,n,0) + \sum_{mn} d_{ssmn}(\lambda)\Pi(s,m,0)\Phi(s,n,0) \\ &+ \sum_{mn} a_{wwmn}(\lambda)\Phi(w,m,0)\Phi(w,n,0) + \sum_{mn} b_{wwmn}(\lambda)\Pi(w,m,0)\Pi(w,n,0) \\ &+ \sum_{mn} c_{wwmn}(\lambda)\Phi(w,m,0)\Pi(w,n,0) + \sum_{mn} d_{wwmn}(\lambda)\Pi(w,m,0)\Phi(w,n,0) \\ &+ \sum_{mn} a_{wsmn}(\lambda)\Phi(w,m,0)\Phi(s,n,0) + \sum_{mn} b_{wsmn}(\lambda)\Pi(w,m,0)\Pi(s,n,0) \\ &+ \sum_{mn} c_{wsmn}(\lambda)\Phi(w,m,0)\Pi(s,n,0) + \sum_{mn} d_{wsmn}(\lambda)\Pi(w,m,0)\Phi(s,n,0) \\ &+ \sum_{mn} a_{swmn}(\lambda)\Phi(s,m,0)\Phi(w,n,0) + \sum_{mn} b_{swmn}(\lambda)\Pi(s,m,0)\Pi(w,n,0) \\ &+ \sum_{mn} c_{swmn}(\lambda)\Phi(s,m,0)\Pi(w,n,0) + \sum_{mn} d_{swmn}(\lambda)\Pi(s,m,0)\Phi(w,n,0). \end{aligned} \tag{39}$$

The initial condition ($\lambda = 0$) corresponds to the original truncated Hamiltonian, including all of the wavelet-scale-coupling terms:

$$\begin{aligned} &a_{ssmn}(0) = \frac{1}{2}(\mu^2\delta_{mn} + D_{ssmn}) \qquad b_{ssmn}(0) = \frac{1}{2}\delta_{mn} \qquad c_{ssmn}(0) = 0 \qquad d_{ssmn}(0) = 0 \\ &a_{wwmn}(0) = \frac{1}{2}(\mu^2\delta_{mn} + D_{wwmn}) \qquad b_{wwmn}(0) = \frac{1}{2}\delta_{mn} \qquad c_{wwmn}(0) = 0 \qquad d_{wwmn}(0) = 0 \\ &a_{wsmn}(0) = D_{wsmn} \qquad b_{wsmn}(0) = 0 \qquad c_{wsmn}(0) = 0 \qquad d_{wsmn}(0) = 0 \\ &a_{swmn}(0) = D_{swmn} \qquad b_{swmn}(0) = 0 \qquad c_{swmn}(0) = 0 \qquad d_{swmn}(0) = 0. \end{aligned}$$

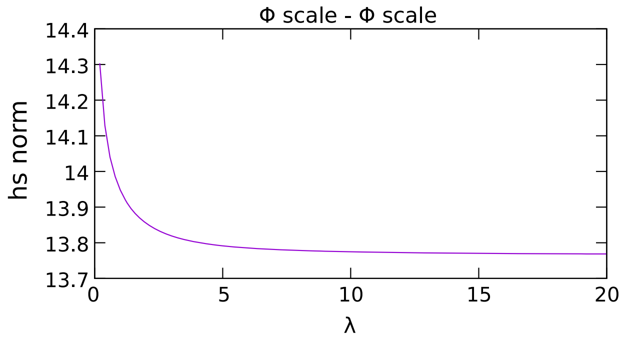

FIG. 1. Hilbert-Schmidt norm: Φ scale-Φ scale.

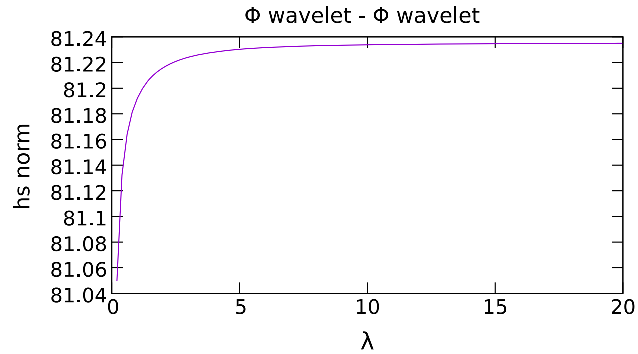

FIG. 2. Hilbert-Schmidt norm: Φ wavelet-Φ wavelet.

To test the flow equation method the mass μ was set to 1. The mass sets the energy scale for the parameter λ. An attempt to solve the flow equation by perturbation theory did not to converge. Convergence was achieved by solving the flow equation using the Euler method, which uses the differential equation to step to successive values of λ. The step size was determined by examining the size and number of matrix elements, to ensure that the errors remain small. A step size of 0.001 was used in our calculations. While the efficiency could be improved with a higher-order solution method, in this test the Euler method was sufficient to see the that flow equation drives the coupling term to zero.

To illustrate the evolution of the coefficients in the expansion (39) we plot the Hilbert-Schmidt norms of the nonzero coefficients

$$\sqrt{\sum_{ij} a^*_{xyij} a_{xyji}} \quad \sqrt{\sum_{ij} b^*_{xyij} b_{xyji}} \times \sqrt{\sum_{ij} c^*_{xyij} c_{xyji}} \quad \sqrt{\sum_{ij} d^*_{xyij} d_{xyji}}$$

as functions of λ.

There are four types of operators, $\Phi(s,n,0)$; $\Pi(s,n,0)$; $\Phi(w,m,0)$; and $\Pi(w,m,0)$, leading to 16 types of quadratic expressions. Figures 1–8 show the Hilbert-Schmidt norms of the coefficients of each of the nonzero quadratic expressions as a function of the flow parameter.

The norms of coefficients involving all scaling or all wavelet fields evolve to nonzero values, while the norms of the coupling matrices all evolve to zero. The plots show that initially the size of the coupling terms falls off very fast, but the rate of decrease slows significantly as λ gets larger. For $\lambda = 20$ the Hilbert-Schmidt norms of the coupling coefficients are reduced by about 2 orders of magnitude from their original values.

The Hilbert-Schmidt norms of the coefficients are dominated by the largest matrix elements. It is also useful to understand how the individual matrix coefficients converge.

Figures 9–12 provide a graphical representation of the coefficient matrices for different values of λ. The figures should be viewed as a montage of sixteen 16×16 matrices. Indices 0–15 correspond to $\Phi(s)$, 16–31 correspond to $\Pi(s)$, 32–47 correspond to $\Phi(w)$, and 48–63 correspond to $\Pi(w)$. The gray scale shows the size of the coefficients of the quadratic expressions in the Hamiltonian as a function of λ.

The four figures correspond to different values of the flow parameter: $\lambda = 0$, $\lambda = 0.2$, $\lambda = 2$, and $\lambda = 20$.

Figure 9 represents the initial values. The two narrow diagonal bands in the 16–31 and 48–63 blocks represent the coefficients $b_{ssmn}(0)$ and $b_{wwmn}(0)$ respectively. The fatter diagonal bands in the upper left-hand part of this figure are associated with the scale-scale and wavelet-wavelet

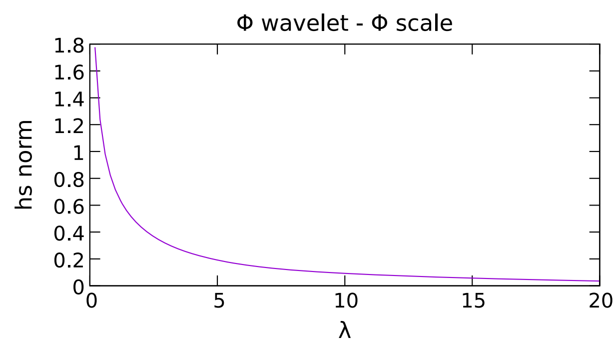

FIG. 3. Hilbert-Schmidt norm: Φ scale-Φ scale.

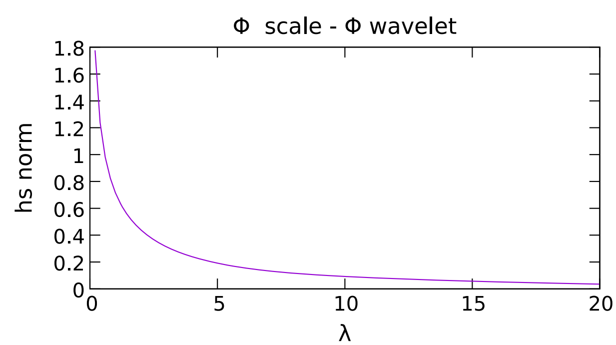

FIG. 4. Hilbert-Schmidt norm: Φ scale-Φ wavelet.

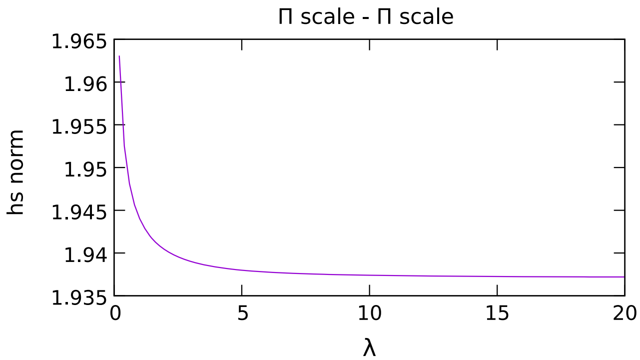

FIG. 5. Hilbert-Schmidt norm: Π scale-Π scale.

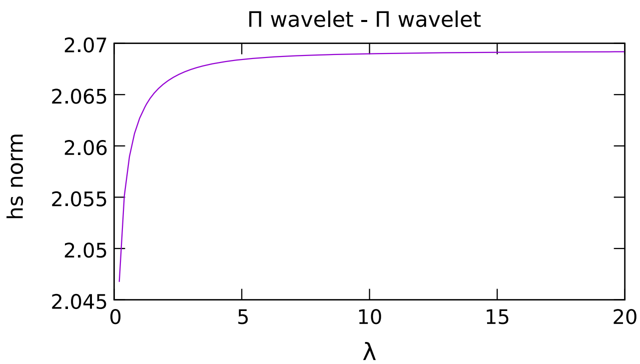

FIG. 6. Hilbert-Schmidt norm: Π wavelet-Π wavelet.

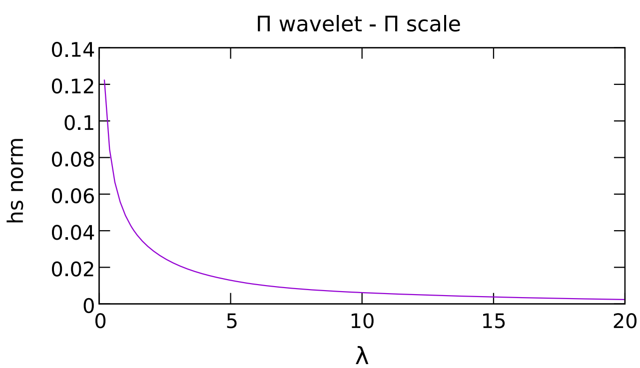

FIG. 7. Hilbert-Schmidt norm: Π wavelet-Π scale.

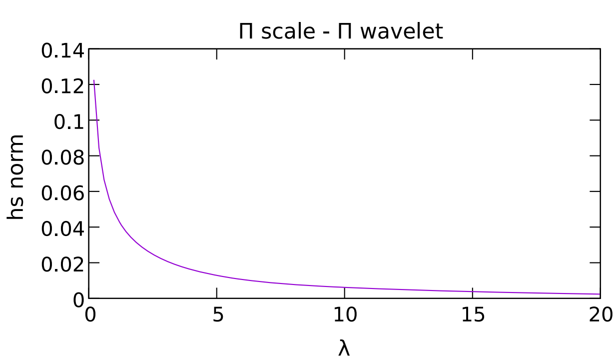

FIG. 8. Hilbert-Schmidt norm: Π scale-Π wavelet.

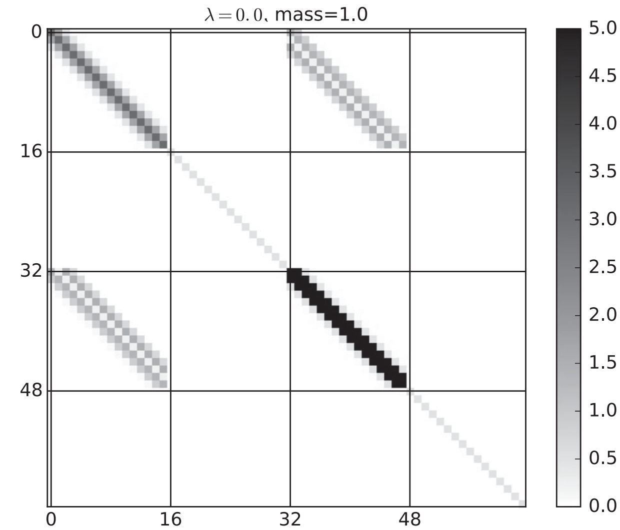

FIG. 9. Full matrix, $\lambda = 0$, mass $= 1$.

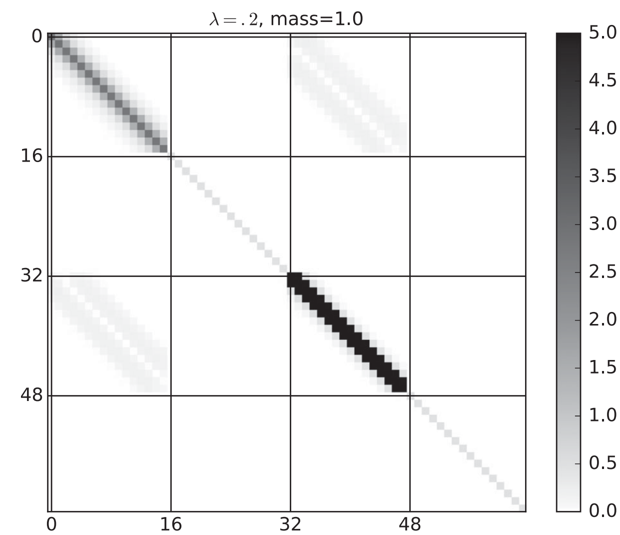

FIG. 10. Full matrix, $\lambda = 0.2$, mass $= 1$.

derivative terms. They are almost diagonal because the matrices $D_{x;mn}$ only couple neighboring degrees of freedom.

The terms above and below the diagonal are the coefficients of the scale-wavelet and wavelet-scale derivative terms, $a_{swmn}(0)$ and $a_{wsmn}(0)$. These are responsible for the coupling of the two scales and are the terms that the flow equation is designed to suppress.

Figure 10 shows the value of these coefficients for $\lambda = 0.2$. For this value of λ the coupling terms have become smaller and more nonlocal. This is because repeated applications of the derivative matrix widen the support of the degrees of freedom that are coupled together.

Figure 11 shows that by $\lambda = 2$ the scale-coupling terms have essentially disappeared.

Figure 12 show that integrating the flow equation out to $\lambda = 20$ does not lead to any big changes. This is consistent

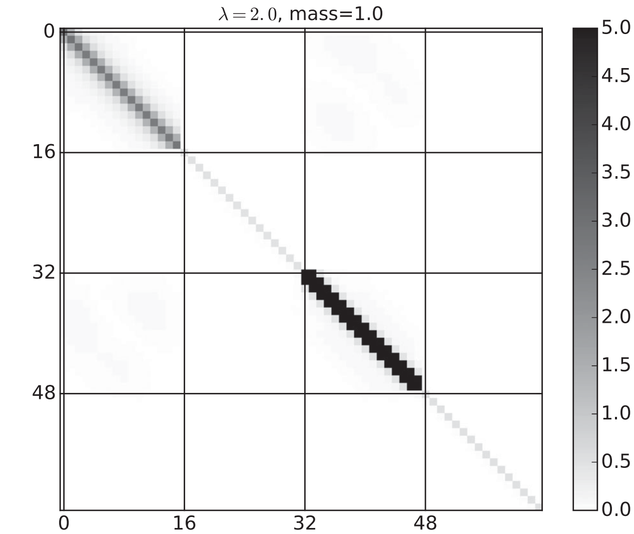

FIG. 11. Full matrix, $\lambda = 2.0$, mass = 1.

with the behavior shown in Figs. 1–8, that the exponential suppression slows as λ is increased. It is worth noting that the width of the diagonal band in the uncoupled Hamiltonian at $\lambda = 20$ is about the same size as the width of the corresponding band in the original Hamiltonian. This shows that at least for this example the flow equation approximately preserves the local nature of the truncated theory.

The figures support the contention that flow equation methods can be successfully applied to separate scales in wavelet discretized field theory.

For any value of the flow parameter the flow equation generates a new equivalent Hamiltonian. Ignoring the small terms that couple the wavelet to the scaling-function fields, the Hamiltonian becomes a sum of two commuting operators that have degrees of freedom associated with different scale degrees of freedom, but each operator includes the effects of the eliminated degrees that appear in the other operator.

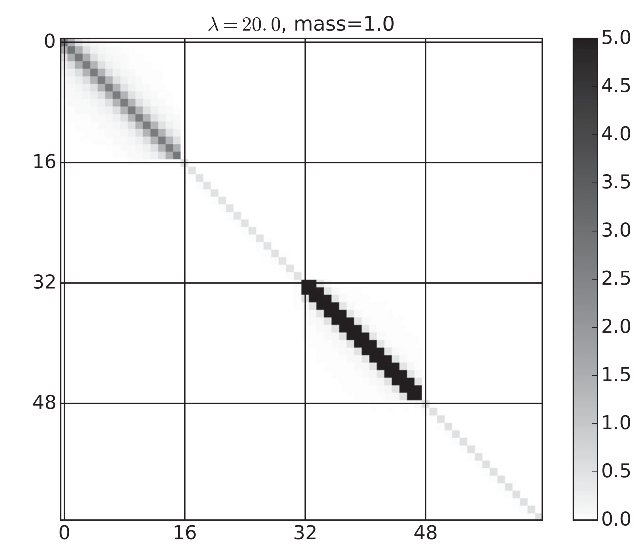

FIG. 12. Full matrix, $\lambda = 20.0$, mass = 1.

In the free-field case the Hamiltonians are quadratic functions of the canonical fields for any value of the flow parameter. For sufficiently large values of the flow parameter the Hamiltonian becomes sums of two Hamiltonians involving different scale degrees of freedom.

It is still necessary to solve for the vacuum and solve the field equations of the truncated theory. In this case there are two independent systems of field equations using the decoupled Hamiltonians:

$$\dot{\Phi}(s,n,t) = i[H_s(\lambda), \Phi(s,n,t)]$$
$$\dot{\Pi}(s,n,t) = i[H_s(\lambda), \Pi(s,n,t)]$$

and

$$\dot{\Phi}(w,n,t) = i[H_w(\lambda), \Phi(w,n,t)]$$
$$\dot{\Pi}(w,n,t) = i[H_w(\lambda), \Pi(w,n,t)].$$

The effective Hamiltonian $H_s(\lambda)$ is the effective Hamiltonian with the relevant (scaling-function) degrees of freedom. For the free field, the dynamics corresponds to a set of coupled Harmonic oscillators. This can be used to solve the Heisenberg equations, compute the vacuum, and compute approximate correlation functions for the coarse scale block Hamiltonian. This is discussed in more detail in the next section.

VI. ANALYSIS

The results of the previous section show that in the free-field case that flow equation methods can be used to approximately block diagonalize the truncated Hamiltonian by scale. To better understand properties of the solution it is helpful to first consider properties of the exact solution of the truncated equations and how they respond to changes in volume and resolution truncations. Volume truncations change the number of canonical pairs of fields while resolution truncations only change the overlap matrices of the spatial derivatives (24)–(26). In general the initial truncated Hamiltonian can be expressed in matrix form as

$$H = \frac{1}{2}\left[(\Pi^s, \Pi^w)\begin{pmatrix} I_s & 0 \\ 0 & I_w \end{pmatrix}\begin{pmatrix} \Pi^s \\ \Pi^w \end{pmatrix} + (\Phi^s, \Phi^w)\begin{pmatrix} \mu^2 I + D_s & D_{sw} \\ D_{ws} & \mu^2 I + D_w \end{pmatrix}\begin{pmatrix} \Phi^s \\ \Phi^w \end{pmatrix}\right]$$

where the upper components represent the scaling-function fields and the lower components represent the wavelet fields. Because the matrix

$$M \coloneqq \begin{pmatrix} \mu^2 I + D_s & D_{sw} \\ D_{ws} & \mu^2 I + D_w \end{pmatrix}$$

is a real symmetric matrix it can be diagonalized by a real orthogonal matrix O:

$$O^t M O = \begin{pmatrix} m^s & 0 \\ 0 & m^w \end{pmatrix} \tag{40}$$

where m^s and m^w are diagonal matrices consisting of eigenvalues of the matrix M.

Transformed discrete fields are defined by

$$\begin{pmatrix} \Phi'^s \\ \Phi'^w \end{pmatrix} \coloneqq O \begin{pmatrix} \Phi^s \\ \Phi^w \end{pmatrix} \quad \text{and} \quad \begin{pmatrix} \Pi'^s \\ \Pi'^w \end{pmatrix} \coloneqq O \begin{pmatrix} \Pi^s \\ \Pi^w \end{pmatrix}.$$

The orthogonality of O implies that the transformed fields satisfy canonical commutation relations. It follows from the Stone–von Neumann uniqueness theorem that this transformation of the field operators can be implemented by a unitary transformation W:

$$W \begin{pmatrix} \Phi^s \\ \Phi^w \end{pmatrix} W^\dagger = \begin{pmatrix} \Phi'^s \\ \Phi'^w \end{pmatrix} = O \begin{pmatrix} \Phi^s \\ \Phi^w \end{pmatrix}$$
$$\text{and} \quad W \begin{pmatrix} \Pi^s \\ \Pi^w \end{pmatrix} W^\dagger = \begin{pmatrix} \Pi'^s \\ \Pi'^w \end{pmatrix}$$
$$= O \begin{pmatrix} \Pi^s \\ \Pi^w \end{pmatrix}.$$

If this transformation is applied to the truncated Hamiltonian it is transformed into the sum of uncoupled harmonic oscillator Hamiltonians, where the squares of the oscillator frequencies are exactly the eigenvalues of the matrix M:

$$H' = UHU^\dagger = \frac{1}{2}\left[(\Pi^s, \Pi^w) \begin{pmatrix} I & 0 \\ 0 & I \end{pmatrix} \begin{pmatrix} \Pi^s \\ \Pi^w \end{pmatrix} + (\Phi^s, \Phi^w) \begin{pmatrix} m^s & 0 \\ 0 & m^w \end{pmatrix} \begin{pmatrix} \Phi^s \\ \Phi^w \end{pmatrix} \right]$$

or

$$H = \frac{1}{2}\sum_n (\Pi(s,n,0)\Pi(s,n,0) + m_n^s \Phi(s,n,0)\Phi(s,n,0)) + \frac{1}{2}\sum_n (\Pi(w,n,0)\Pi(w,n,0) + m_n^w \Phi(w,n,0)\Phi(w,n,0)).$$

The ground state of the truncated Hamiltonian is the state annihilated by the annihilation operators

$$a_n^s \coloneqq \frac{1}{\sqrt{2} m_n^{s\,1/4}} \sum_j (\sqrt{m_n^s}\Phi(s,n,0) + i\Pi(s,n,0)) \tag{41}$$

$$a_n^w \coloneqq \frac{1}{\sqrt{2} m_n^{w\,1/4}} \sum_j (\sqrt{m_n^w}\Phi(w,n,0) + i\Pi(w,n,0)) \tag{42}$$

where m_n^s and m_n^w are the eigenvalues of the diagonal matrices m^s and m^w. It follows that the unitary operator U does a complete diagonalization that separates different scale degrees of freedom. The transformation O is not unique, since permutations of the columns of O permute the eigenvalues. This means that the identification of a given oscillator frequency with a wavelet or scaling-function degree of freedom depends on the choice of O.

The advantage of this representation is that it can be used to understand the behavior of the truncated Hamiltonian with respect to changes in volume and resolution as well as the role of the mass parameter. The key observation is that the truncated system is equivalent to a set of uncoupled harmonic oscillators where (1) the number of oscillators is proportional to the cutoff volume and the oscillator frequencies are square roots of the eigenvalues of the matrix M. The matrix M is $\mu^2 I + D$, where D is a positive symmetric matrix with eigenvalues d_i. The matrix D is the only quantity in the truncated Hamiltonian that changes under scale changes. If we double the resolution, $D \to 4D$. This means that the eigenvalues of M have the form $m_i = \mu^2 + d_i$ and under a change of resolution by a factor of 2 they become $m_i \to \mu^2 + 4d_i$. This means that doubling the resolution increases the separation between the squares of the oscillator frequencies by a factor of 4. The other property of D is that, up to boundary terms, it is translationally invariant. If we think of it as representing the kinetic energy of particles in a box, we expect that doubling the box size will introduce new modes with half of the frequency. Thus, while increasing the resolution increases the separation between oscillator frequencies, if the volume is increased, new lower-frequency modes are added that fill in the gaps generated by increasing the resolution. The mass μ provides a lower bound for the oscillator frequencies. Since the spectrum of the exact free-field Hamiltonian is continuous, in order to get a continuum limit, it is necessary to simultaneously increase both the volume and resolution in a manner that the separation between adjacent normal mode frequencies vanishes.

The resolution for a fixed scale can also be improved by increasing the order K of the scaling-function-wavelet basis. For a fixed scale, basis functions with higher values of K can locally pointwise represent higher-degree polynomials than the $K = 3$ basis functions [51]. The cost is that the basis functions have larger support and are thus less local for a given level of truncation. The improvement in efficiency by increasing K for a fixed-scale wavelet-truncated free-field theory was demonstrated in [20].

It is also interesting to note that the scaling properties of the Hamiltonian can be misleading. Specifically, for the free-field Hamiltonian, in the infinite-resolution limit it looks like the matrix $D \to 4^k D$ which should eventually dominate the fixed mass for large k. However it is clear that the mass cannot be ignored, since it fixes the minimum value of the energies for any scale. This suggest that it might be more useful to consider the properties' correlation functions under change of volume and scale, since these quantities also depend on the vacuum. These issues will clearly become more complex for interacting theories. The correlation function (Wightman function) for the discrete field is

$$\begin{aligned}\langle 0|\Phi(x,t_x)\Phi(y,t_y)|0\rangle \\ &= \langle 0'|\Phi'(x)\Phi'(y)|0'\rangle \\ &= \sum_{mnk} s_n(x) s_m(y) O_{nk} O_{mk} \frac{1}{2\sqrt{m_k}} e^{im_k(t_y-t_x)}.\end{aligned}$$

These are discussed in [20].

The discussion above does not directly apply to the block diagonal Hamiltonian constructed by the flow equation; however the transformation $U(\lambda)$ generated by the flow cannot change the spectrum of the Hamiltonian. It can only determine which of the exact eigenvalues get assigned to each of the two blocks. The scaling properties of the eigenvalues are the same as in the exact case.

We can understand what happens in the flow equation case. For mass $\mu = 1$ and $\lambda = 20$ the coefficients b_{ssmn} and b_{wwmn} are within about 2% of their initial values. This means that the squares of the normal mode frequencies of the scaling block diagonal Hamiltonian are approximately eigenvalues of the matrix $2a_{ssmn}(\lambda = 20)$. These can be compared to the corresponding normal mode frequencies of the full truncated Hamiltonian.

In Table II we display the squares of the $\lambda = 20$ normal mode frequencies in column 1, the squares of the normal mode frequencies of the Hamiltonian obtained by simply throwing away the wavelet degrees of freedom without eliminating them in column 2, and the squares of the normal mode frequencies of the full truncated Hamiltonian in columns 3 and 4. Inspection of this table shows that the frequencies in the first column are approximately equal to the frequencies in the third column. This shows that the flow equation block diagonalizes the Hamiltonian into a block with the 16 lowest-frequency modes (the coarse scale block) and another block with the 16 highest-frequency modes (fine scale block). The properties of these matrices under change of scale or resolution follow from the behavior of the normal mode frequencies—increasing the volume adds more low-frequency modes, while increasing the resolution increases the separation between the different normal mode frequencies. The mass sets the lowest normal mode frequency.

In this work only two scales that differ by a factor of 2 were considered. Flow equation methods easily generalize to treat truncated theories with many different scales. While the goal of this paper was to construct an equivalent effective theory by eliminating fine-resolution degrees of freedom that are not explicitly needed, the calculation is equivalent to either truncating the Hamiltonian using a fixed fine-scale truncated Hamiltonian of the form (23) or using the equivalence (9) of the fine-scale truncated Hamiltonian to the multiscale truncated Hamiltonian (22). This is a canonical transformation that can be realized unitarily. In this work the fine- and coarse-scale degrees of freedom are decoupled. In [20] the other two equivalent representations are used. They interpret the relation between the fine-scale scaling-function representation and the multiscale scaling-function-wavelet representation, which is given by the wavelet transform, as an explicit example of an AdS-CFT-like bulk boundary duality, where the multiple scales in the multiscale Hamiltonian (22) represent the discretization of an extra dimension. For the free-field example, at a given level of fine scale and volume truncation, all three Hamiltonians represent coupled oscillators with the same normal mode frequencies.

Each of these representations has different advantages. The representation discussed in this work is focused on developing a formulation of the theory using only degrees of freedom on one coarse scale, which would ideally be identified with a physical scale. The multiscale representation has the advantage that it initially leads to a discrete representation of the exact (untruncated) theory that can be subsequently truncated. The direct fine scale truncations are similar to lattice truncations. While they are never exact, the scaling properties of the basis functions make this representation the most natural one to study the limit to an arbitrarily fine resolution. This is done explicitly in [20] where the truncated Daubechies' free-field scaling-wavelet vacuum correlation functions in both the massive and massless case are shown to converge to the corresponding free-field Wightman functions in [20].

TABLE II. Normal mode frequencies

$\lambda = 20$, $\mu = 1$	Truncated	Exact 1:16	Exact 17:32
1.037	1.037	1.041	16.65
1.145	1.146	1.153	19.25
1.326	1.333	1.340	22.08
1.583	1.609	1.604	25.12
1.919	1.995	1.947	28.34
2.341	2.525	2.373	31.67
2.861	3.236	2.890	35.07
3.493	4.161	3.508	38.46
4.263	5.317	4.243	41.78
5.201	6.689	5.112	44.95
6.346	8.232	6.134	47.89
7.722	9.859	7.332	50.53
9.309	11.45	8.729	52.79
11.02	12.89	10.34	54.62
12.74	14.03	12.19	55.97
14.35	14.76	14.29	56.79

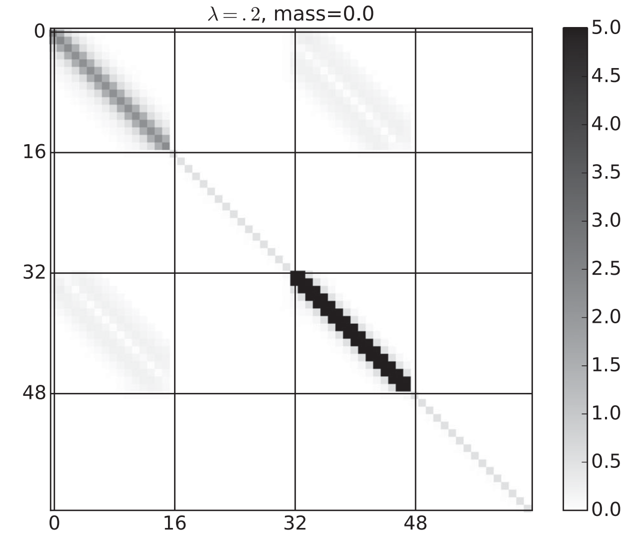

FIG. 13. Full matrix, $\lambda = 0.2$, mass $= 0$.

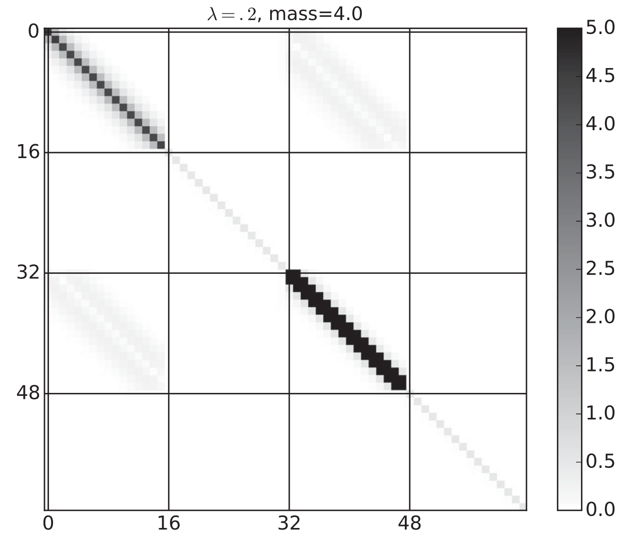

FIG. 15. Full matrix, $\lambda = 0.2$, mass $= 4$.

The one thing that was not discussed is what happens to the numerical methods when the mass is changed. In this free-field example the mass fixes the lower limit of the spectrum and also fixes the dimensions of the flow parameter. One might expect that since the exponential falloff in (34) is determined by the separation of the evolved normal mode eigenvalues of the block diagonal part of the Hamiltonian, that the convergence of the flow equation will not be significantly affected by changing the mass. To test this we solved the flow equation for $\mu^2 = 0$ and $\mu^2 = 16$ for $\lambda = 0.2$ and $\lambda = 2$. The results are shown in Figs. 13–16. These figures look very similar to the matrices in Figs. 10 and 11 for $\mu^2 = 1$. This suggests that the flow equation has no special difficulties in treating truncated theories even when $m = 0$.

VII. SUMMARY, CONCLUSIONS AND OUTLOOK

The purpose of this work is to examine the use of flow equation methods to separate the physics on different resolution scales in an exact wavelet discretization of quantum field theory. While quantum field theory couples all distance scales, there is a physically relevant scale (or resolution) and it is desirable to formulate the theory directly in terms of the degrees of freedom associated with the physically relevant degrees of freedom. This can be done by eliminating the short-distance degrees of freedom.

While it may not be possible to get a well-defined local theory by eliminating all arbitrarily small distance degrees of freedom, it is possible formulate an effective theory that includes the important short-distance physics by

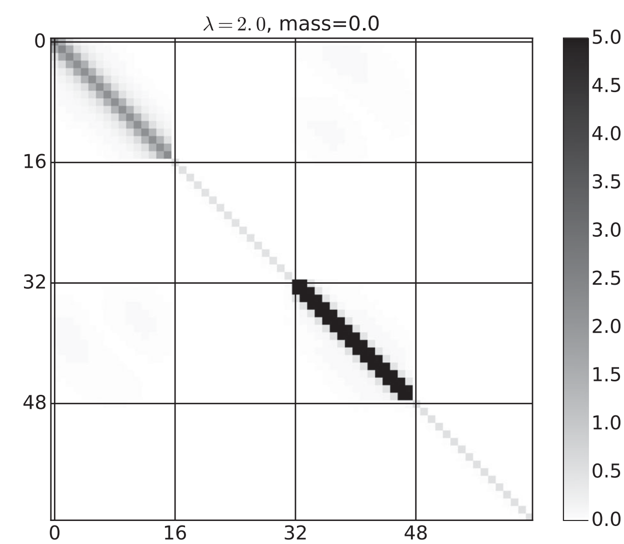

FIG. 14. Full matrix, $\lambda = 2.0$, mass $= 0$.

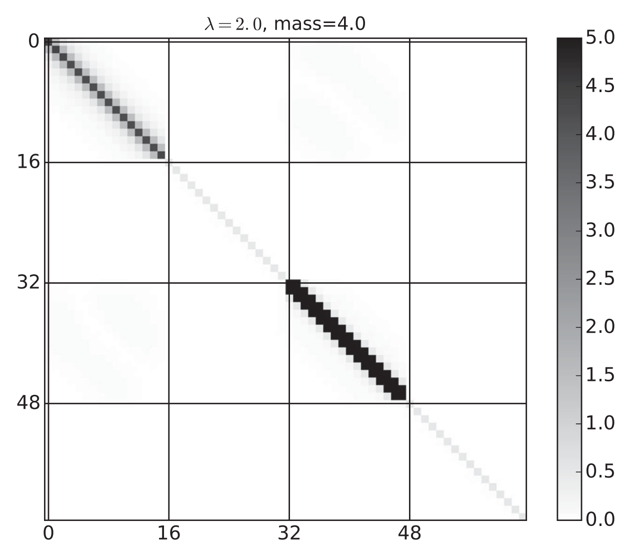

FIG. 16. Full matrix, $\lambda = 2.0$, mass $= 4$.

eliminating degrees of freedom between the physically relevant scale and a chosen minimal resolution scale. The justification for this is that for a given application there is a relevant volume and energy scale. These restrictions generally imply that the dynamics is dominated by a finite number of degrees of freedom. This can be understood in a number of ways. For a free-field theory restricting the energy leads to a subspace of the Fock space with an upper bound on the number of particles. If this system is put in a finite volume, the free particles in a finite volume have discrete energies and only a finite number of these states have energy less than the energy scale. These degrees of freedom are sufficient to formulate the dynamics relevant to the system.

In the scaling-wavelet representation this provides a justification for a volume/resolution truncation of the field theory. The smallest scales that influence the physics can be eliminated by block diagonalizing the Hamiltonian. In this representation the field was expressed as a linear combination of almost local operators classified by position and resolution.

These operators satisfy simple discrete canonical commutation relations. In this representation the exact Hamiltonian is a finite-degree polynomial with known constant coefficients in an infinite number of these operators. Resolution and volume truncations lead to truncated Hamiltonians involving a finite number of degrees of freedom.

The approach taken in this paper differs from other wavelet approaches to quantum field theory [2,4] [8–10,12, 13,16]. The basis functions that are used in this work are orthonormal with compact support, but they have a limited amount of smoothness. In most wavelet approaches the wavelet functions are overcomplete, smooth functions that do not have compact support. The justification for smearing fields with functions that have a limited amount of smoothness is that when these basis functions are integrated against free-field Wightman functions the results are well defined. This means the resulting operators are well defined on the free-field Fock space, and for theories truncated to a finite number of degrees of freedom it is not necessary to pass to an inequivalent representation of the field algebra in order to solve the field equations.

While there are a number of potential methods to eliminate the short-distance degrees of freedom, the simple nature of the commutation relations of the discrete field operators suggests using flow equation methods, where the generator of the desired unitary transformation involves commutators of products of canonical pairs of operators. These methods have been proposed to be used in QCD [39–41], as well as in potential theory [44–46]. Those applications focus on momentum scales and the equations are designed to drive the Hamiltonian to a diagonal form. In this work the goal is to formulate the problem in terms of distance scales and to block diagonalize [42] the Hamiltonian rather than diagonalize it. In this example the transformed theory consists of two sets of a canonically conjugate set of operators that operate on different distance scales. The generator of the flow equation is chosen to eliminate the terms that couple these scales in the Hamiltonian.

This method was tested using the Hamiltonian for a free scalar field. While the free field is trivial, in the wavelet representation the space derivatives in the Hamiltonian generate nontrivial terms that couple the degrees of freedom on different scales. This Hamiltonian has the advantage that the flow equation applied to this Hamiltonian does not generate an infinite number of new types of many-body operators. This allows us to focus on testing the flow equation as a method to separate scales without the complication of understanding the relative importance of the generated interactions. What we found can be summarized by the following observations:

(1) It was demonstrated that flow equation methods with a suitable generator could be used to separate scales in a wavelet truncated theory.
(2) The truncated free-field Hamiltonian is equivalent to a system of coupled harmonic oscillators. The flow equation block diagonalized the Hamiltonian with the coarse-scale block containing the 16 lowest-frequency normal modes and the fine-scale block containing the 16 highest-frequency modes.
(3) Increasing the truncated volume generated new low-frequency modes, while increasing the resolution increased the separation between modes. The mass set a lower bound on the normal mode frequencies.
(4) The flow equation exhibited convergence for masses between 0 and 4.
(5) For this problem, the flow equation was successfully applied directly to the Hamiltonian, without projecting on a subspace.
(6) We found the that flow equation could be integrated using the Euler method, but perturbation theory failed to converge.
(7) The evolved Hamiltonian was approximately local.
(8) The spectral properties suggest the in order to approach the continuous spectrum of the exact theory, the volume and resolution truncations need to be removed together.
(9) In our test the coefficients of the coupling terms initially fell off quickly, but the rate of falloff slowed down significantly as the flow parameter increased. The method reduced the coupling coefficients by a factor of about 100 for a modest value of the flow parameter.

The next step in this program is to consider models with interactions and to consider models in $3+1$ dimensions. The complication with interactions is that integrating the flow equation generates new operators with each step of the Euler method. A different flow generator will need to be formulated in order to get results comparable to the results outlined above. This is because the analysis that led to (33)–(34) does not apply to the interacting case. On the other hand, the truncations suggest that in the interacting case only a finite-dimensional subspace of the Fock space is relevant. Flow equation methods are more naturally designed to work on subspaces and diagonalize or block diagonalize operators projected on subspaces. These projections limit the types and nature of the many-body operators that are generated by solving the flow equations. Generalizations to $3+1$ dimensions are straightforward. Single basis functions are replaced by products of three basis functions. While the bookkeeping becomes more difficult, the basic structure is essentially unchanged.

ACKNOWLEDGMENTS

The authors would like to thank Robert Perry and Mikhail Altaisky for valuable feedback on this work. We are also indebted to the referee, who provided additional feedback and who pointed out the elegant method form computing the overlap integrals due to Beylkin. This work was performed under the auspices of the U. S. Department of Energy, Office of Nuclear Physics, Award No. DE-SC0016457 with the University of Iowa.

APPENDIX: COMPUTATION OF OVERLAP INTEGRALS

The Daubechies wavelets and scaling functions are fractal functions. Integrals involving these functions cannot be computed using conventional methods; however the scaling equation (1) and normalization condition (2) lead to linear constraints that reduce the exact integration of all of the relevant integrals to finite linear algebra.

These integrals were computed in [11]. In this Appendix we calculate them using a method introduced by Beylkin [27]. While the equations are identical to Beylkin's, we derive them without computing second derivatives of the $K=3$ scaling functions, which only have continuous first derivatives.

Repeated application of the scaling equation (1) and the definition of the mother wavelet (11) can be used to express the coefficients $D^k_{s;mn}$, $D^{kl}_{sw;mn}$, and $D^{w;jl}_{mn}$ in terms of $D^0_{s;mn}$ and the h_l in Table I:

$$D^k_{s;mn} = \int s^{k\prime}_m(x) s^{k\prime}_n(x)dx$$

$$= 2^{2k}\int s'(x-m)s'(x-n) = 2^k D^0_{s;mn}$$

$$D^{kl}_{sw;mn} = \int s^{k\prime}_m(x) w^{l\prime}_n(x)dx$$

$$= 2^{2(l+1)}\sum_{m'n'} H^{l+1-k}_{mm'} G_{nn'} D^0_{s;m'n'}$$

$$D^{w;jl}_{mn} = \int w^{j\prime}_m(x) w^{l\prime}_n(x)dx$$

$$= 2^{2(l+1)}\sum_{m'n'} (GH^{l-j})_{mm'} G_{nn'} D^0_{s;m'n'} \qquad (l\geq j)$$

where the primes denote derivatives, the matrices H_{mn} and G_{mn} are defined in terms of the scaling-function and wavelet weights by

$$H_{mn} = h_{n-2m} \qquad G_{mn} = g_{n-2m}$$

and

$$D^0_{s;mn} = \int s'_m(x) s'_n(x)dx.$$

Translational invariance implies that $D^0_{s;mn}$ can be expressed in terms of

$$D^0_{s;mn} = D^0_{s;0,n-m}.$$

For $K=3$ there are nine nonzero coefficients

$$D^0_{s;0m} \coloneqq \int s'(x)s'(x-m)dx \qquad -4\leq m\leq 4. \tag{A1}$$

Letting $x'=x-m$ gives $D^0_{s;0-m} = D^0_{s;0m}$ so there are only five independent integrals that need to be evaluated. Differentiating the scaling equation (1) gives a renormalization group equation for the derivatives

$$s'(x-m) = 2\sqrt{2}\sum_l h_l s'(2x-2m-l). \tag{A2}$$

Using (A2) in (A1) gives homogeneous equations relating the nonzero $D^0_{s;0m}$'s:

$$D^0_{s;0m} = 4\sum_{l,n} h_l h_{l+n} D^0_{s;02m+n}. \tag{A3}$$

The coefficients

$$a_n \coloneqq 2\sum_l h_l h_{l+n}$$

are called autocorrelation coefficients. It follows from the orthogonality constraint on translations of the scaling function (4) that $a_0 = 2.0$ and $a_{2n}=0$ for $n\neq 0$. The remaining autocorrelation coefficients for odd n are rational. For the Daubechies $K=3$ h_l in Table I the nonzero autocorrelation coefficients can be computed and they are

$$a_0 = 2 \qquad a_1 = a_{-1} = \frac{75}{64} \qquad a_3 = a_{-3} = -\frac{25}{128}$$

$$a_5 = a_{-5} = \frac{3}{128}.$$

The homogeneous equation (A3) can be expressed in terms of a_n:

$$D^0_{s;0m} = \sum 2a_n D^0_{s;02m+n}. \tag{A4}$$

In order to solve this system for $D^0_{s;0m}$ an inhomogeneous equation is needed. To derive an inhomogeneous equation note that for $K = 3$, 1, x and x^2 can be expressed pointwise as locally finite expansions in the scaling functions. The expansions have the form

$$1 = \sum_n s_n(x) \tag{A5}$$

$$x = \sum_n (n + \langle x \rangle) s_n(x) \tag{A6}$$

$$x^2 = \sum_n (n^2 + 2n\langle x \rangle + \langle x^2 \rangle) s_n(x) \tag{A7}$$

where $\langle x^n \rangle = \int s(x) x^n$ are moments of the scaling function. While the moments can also be computed exactly, they are not needed to calculate $D^0_{s;0m}$. Differentiating (A6), using (A5), gives

$$1 = \sum_n n s'_n(x).$$

Differentiating (A7) using (A6) gives

$$2x = \sum_n (n^2 + 2n\langle x \rangle) s'_n(x) = \sum_n n^2 s'_n(x) + 2\langle x \rangle.$$

Multiplying by $s'(x)$ and integrating gives

$$\begin{aligned} \int 2xs'(x) &= -2 \\ &= \sum_n n^2 \int s'_n(x) s'(x) dx + 2\langle x \rangle \int s'(x) dx \\ &= \sum_n n^2 \int s'_n(x) s'(x) dx. \end{aligned}$$

This gives the inhomogeneous equation

$$\sum_n n^2 D^0_{s;n0} = -2. \tag{A8}$$

The linear system consisting of Eqs. (A4) and (A8) has rational coefficients and can be solved exactly for rational solutions:

$$\begin{aligned} D^0_{s;40} &= D^0_{s;-40} = -3/560 \\ D^0_{s;30} &= D^0_{s;-30} = -4/35 \\ D^0_{s;20} &= D^0_{s;-20} = 92/105 \\ D^0_{s;10} &= D^0_{s;-10} = -356/105 \\ D^0_{s;00} &= 295/56. \end{aligned}$$

Similar methods [32] can be used to compute the overlap integrals (27) that appear in interacting theories.

[1] C. Best and A. Schaefer, arXiv:hep-lat/9402012.
[2] P. Federbush, Prog. Theor. Phys. **94**, 1135 (1995).
[3] I. G. Halliday and P. Suranyi, Nucl. Phys. **B436**, 414 (1995).
[4] G. Battle, *Wavelets and Renormalization*, Series in Approximations and Decompositions Volume 10 (World Scientific, Singapore, 1999).
[5] C. Best, Nucl. Phys. B, Proc. Suppl. **83**, 848 (2000).
[6] A. E. Ismail, G. C. Rutledge, and G. Stephanopoulos, J. Chem. Phys. **118**, 4414 (2003).
[7] A. E. Ismail, G. C. Rutledge, and G. Stephanopoulos, J. Chem. Phys. **118**, 4424 (2003).
[8] M. V. Altaisky, SIGMA **3**, 105 (2007).
[9] S. Albeverio and M. V. Altaisky, arXiv:0901.2806v2.
[10] M. V. Altaisky, Phys. Rev. D **81**, 125003 (2010).
[11] F. Bulut and W. N. Polyzou, Phys. Rev. D **87**, 116011 (2013).
[12] M. V. Altaisky and N. E. Kaputkina, Phys. Rev. D **88**, 025015 (2013).
[13] M. V. Altaisky and N. E. Kaputkina, Izv. Vuz. Fiz. **10**, 68 (2012) [Russ. Phys. J. **55**, 1177 (2013)].
[14] W. N. Polyzou and F. Bulut, Few-Body Syst. **55**, 561 (2014).
[15] Gavin K. Brennen, Peter Rohde, Barry C. Sanders, and Sukhwinder Singh, Phys. Rev. A **92**, 032315 (2015).
[16] M. V. Altaisky, Phys. Rev. D **93**, 105043 (2016).
[17] M. V. Altaisky and N. E. Kaputkina, Int. J. Theor. Phys. **55**, 2805 (2016).
[18] M. V. Altaisky, Phys. Rev. D **93**, 105043 (2016).
[19] G. Evenbly and S. R. White, Phys. Rev. Lett. **116**, 140403 (2016).
[20] S. Singh and G. K. Brennen, arXiv:1606.05068.
[21] I. Daubechies, Commun. Pure Appl. Math. **41**, 909 (1988).
[22] I. Daubechies, *Ten Lectures on Wavelets*, CBMS-NSF Regional Conference Series in Applied Mathematics (SIAM, Philadelphia, 1992).
[23] A. Latto, H. L. Resnikoff, and E. Tenenbaum, *Proceedings of the French-USA Workshop on Wavelets and Turbulence* (Springer, New York, 1991).
[24] A. Latto and E. Tenenbaum, *Comptes Rendus de l'Académie des Sciences*, Mathématique Série I (Elsevier, New York, 1990), Vol. 311, pp. 903–909.
[25] G. Beylkin, SIAM J. Numer. Anal. **29**, 1716 (1992).
[26] G. Beylkin and N. Saito, Proc. SPIE Int. Soc. Opt. Eng. **1826**, 39 (1992).

[27] G. Beylkin, SIAM J. Numer. Anal. **29**, 1716 (1992).
[28] N. Saito and G. Beylkin, IEEE Trans. Signal Process. **41**, 3584 (1993).
[29] G. Kaiser, *A Friendly Guide to Wavelets* (Birkhauser, Boston, 1994).
[30] H. L. Resnikoff and R. O. Wells, Jr., *Wavelet Analysis* (Springer, New York, 1998).
[31] O. Bratteli and P. Jorgensen, *Wavelets through a Looking Glass: The World of the Spectrum* (Birkhäuser, Boston, 2002).
[32] B. M. Kessler, G. L. Payne, and W. N. Polyzou, arXiv: nucl-th/0305025v2.
[33] B. M. Kessler, G. L. Payne, and W. N. Polyzou, Few-Body Syst. **33**, 1 (2003).
[34] B. M. Kessler, G. L. Payne, and W. N. Polyzou, Phys. Rev. C **70**, 034003 (2004).
[35] F. Bulut and W. N. Polyzou, Phys. Rev. C **73**, e024003 (2006).
[36] W. Glöckle and L. Müller, Phys. Rev. C **23**, 1183 (1981).
[37] S. Okubo, Prog. Theor. Phys. **12**, 603 (1954).
[38] F. Wegner, Ann. Phys. (Berlin) **506**, 77 (1994).
[39] S. D. Głazek and K. G. Wilson, Phys. Rev. D **48**, 5863 (1993).
[40] S. D. Głazek and K. G. Wilson, Phys. Rev. D **49**, 4214 (1994).
[41] R. J. Perry, Ann. Phys. (N.Y.) **232**, 116 (1994).
[42] B. Bartlett, M.S. thesis, University of Stellenbosch, 2003.
[43] S. Kehrein, *The Flow Equation Approach to Many-Particle Systems* (Springer, Berlin-Heidelberg, 2006).
[44] S. K. Bogner, R. J. Furnstahl, and R. J. Perry, Phys. Rev. C **75**, 061001 (2007).
[45] E. Anderson, S. K. Bogner, R. J. Furnstahl, E. D. Jurgenson, R. J. Perry, and A. Schwenk, Phys. Rev. C **77**, 037001 (2008).
[46] S. K. Bogner, R. J. Furnstahl, and A. Schwenk, Prog. Part. Nucl. Phys. **65**, 94 (2010).
[47] N. N. Bogoliubov and V. Shirkov, *Introduction to the Theory of Quantized Fields* (Wiley, New York, London, Sydney, Toronto, 1959), p. 150.
[48] M. H. Stone, Proc. Natl. Acad. Sci. U.S.A. **16**, 172 (1930).
[49] J. von Neumann, Math. Ann. **104**, 570 (1931); reprinted inJ. von Neumann, *Collected Works*, edited by A. H. Taub (Pergamon Press, New York and Oxford, 1961), Vol. 2, pp. 220–229.
[50] P. A. Perry, *Scattering Theory by the Enss Method*, Reports in Mathematics Vol. 1, edited by J. Dieudonne and Barry Simon (Harwood Academic Publishers, New York, 1983).
[51] G. Beylkin and J. M. Keiser, in *Multiscale Wavelet Methods for PDEs*, edited by W. Dahmen, A. J. Kurdila, and P. Oswald (Academic Press, New York, 1997), pp. 137–197.